THE JOURNAL OF PHYSICAL CHEMISTRY C
A JOURNAL OF THE AMERICAN CHEMICAL SOCIETY

pubs.acs.org/JPCC

Article

Chemical Probing of Water-Stable Methyl Species in Atomic Layer Deposition of Al_2O_3 from Trimethylaluminum and Water

Zhenyu Jin, Suhyun Lee, Seokhee Shin, Da-Som Shin, Hyeri Choi, and Yo-Sep Min*

Cite This: J. Phys. Chem. C 2021, 125, 21434–21442

Read Online

ACCESS | Metrics & More | Article Recommendations | Supporting Information

ABSTRACT: In atomic layer deposition (ALD) of Al_2O_3 thin films using trimethylaluminum (TMA) and water, it is generally believed that the surface methyl species formed by chemical adsorption of TMA are sufficiently water-reactive to produce surface hydroxyls. However, recently, there have been several reports on the presence of persistent methyl species in the water exposure step during the Al_2O_3 ALD process. Here, we performed in situ Fourier-transform infrared spectroscopic analysis to provide evidence that the surface methylated by TMA retains the water-stable methyl species on the surface after exposure to water. The C−H stretching mode of the water-stable methyl species appears at ∼2960 cm^{-1} with a higher wavenumber compared to that of the reactive methyl species (∼2940 cm^{-1}). Furthermore, the water-stable (persistent) methyl species can be chemically probed with ozone (O_3) because ozone reacts with the persistent methyl species to form formate species. During the chemical probing by exposing the persistent methyl species to ozone, the C−H stretching mode of the persistent methyl species disappears at ∼2960 cm^{-1} and the asymmetric stretching mode of the formate species is observed at ∼1609 cm^{-1}. This reveals that the persistent methyl groups are consumed to form the formate species by the chemical probing with ozone. In addition, we propose a plausible reaction between the surface formate species and TMA, which may explain the observations made by the in situ FTIR investigation.

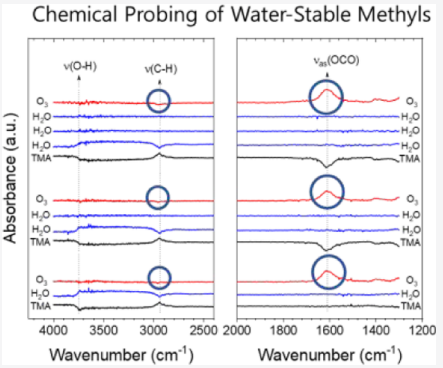

INTRODUCTION

Atomic layer deposition (ALD) is a thin film deposition technique based on alternate chemical adsorption of precursor molecules.[1] Owing to its atomic-scale controllability in conformal growth through self-limiting chemisorption, the ALD method has become one of the indispensable semiconductor-processing technologies for state-of-the-art transistors and memory devices.[2]

Al_2O_3 ALD from trimethylaluminum (TMA) and water is one of the most studied ALD methods,[3] whose overall reaction is

$$Al(CH_3)_3(g) + 3/2H_2O(g) \rightarrow 1/2Al_2O_3(s) + 3CH_4(g) \quad (1)$$

In the practical process of the TMA/H_2O chemistry, TMA and water are alternately exposed to a substrate, and each exposure step of precursors is separated by a purging step with inert gases such as argon and nitrogen gases. Therefore, it is generally believed that the overall reaction of Al_2O_3 growth can be divided into two half-reactions as below

$$n\text{-}OH(s) + Al(CH_3)_3(g) \rightarrow (-O-)_nAl(CH_3)_{3-n}(s) + nCH_4(g) \quad (2a)$$

$$(-O-)_nAl(CH_3)_{3-n}(s) + 3/2H_2O(g) \rightarrow AlO_{3/2}(OH)_n(s) + (3-n)CH_4(g) \quad (2b)$$

where the first (eq 2a) and second (eq 2b) half-reactions correspond to the exposure of TMA and water vapor, respectively. The mechanisms of two half-reactions via a ligand exchange reaction have been studied and verified through in situ analyses[4−8] using a quartz crystal microbalance, quadrupole mass spectrometry, and Fourier-transform infrared spectroscopy (FTIR). A quantum chemical approach using density functional theory (DFT) calculations has also been utilized to provide insights into the understanding of mechanisms.[9−15]

According to the generally accepted mechanism (eqs 2a and 2b), the surface methyl species are believed to be highly reactive toward water for the ligand exchange reaction. However, Frank et al. reported water-stable surface methyl species bonded to Si atoms in their in situ IR study of Al_2O_3 ALD on H-terminated Si(100).[6] The vibrational modes

Received: July 1, 2021
Revised: September 16, 2021
Published: September 28, 2021

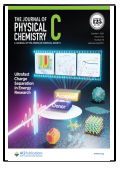

https://doi.org/10.1021/acs.jpcc.1c05889
J. Phys. Chem. C 2021, 125, 21434−21442

(~1270 and 2958 cm^{-1}) of the $SiCH_3$ surface species, which are formed during the first TMA exposure, do not disappear in the subsequent water exposure. Levrau et al. also reported the formation of $SiCH_3$ surface groups, which are not removed upon exposure to water in thermal ALD of Al_2O_3 on porous silica.[16] In the previous DFT investigation by Sandupatla et al., the formation of $SiCH_3$ surface species is found to be possible only on the less-hydroxylated silica surface during the first TMA exposure.[17] They found that these $SiCH_3$ species are rather unreactive toward water due to a high activation energy (196 kJ/mol) of the ligand exchange reaction with water. As a plausible pathway for the formation of the $SiCH_3$ species, several groups have proposed a rearrangement of the methyl groups bonded to Al atoms, via the methyl transfer to siloxane bridges (the case of M = Si in Scheme 1).[18−20]

Scheme 1. Methyl Transfer Reaction of Dimethylaluminum Surface Species on Silica (M = Si) or Alumina (M = Al)[18−20]

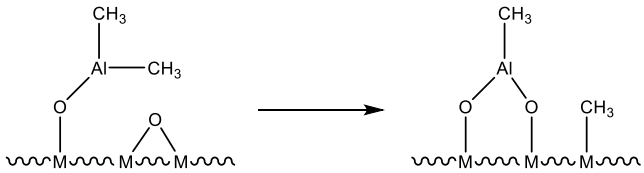

In Scheme 1, the formation of the M-CH_3 species via the methyl transfer may be possible not only on silica but also on alumina. George et al. proposed the methyl transfer reaction (the case of M = Al in Scheme 1) on a hydroxylated surface with a low Al−OH coverage during the TMA exposure of Al_2O_3 ALD.[20] According to their proposal in a mechanistic study of ALD using in situ FTIR spectroscopy, for low Al−OH coverages, isolated Al−OH species exists and reacts with TMA to form Al−O−$Al(CH_3)_2$ (dimethylaluminum, DMA) surface species liberating methane gas (the case of n = 1 in the reaction of eq 2a). Subsequently, the DMA species undergoes the methyl transfer reaction with Al−O−Al in its vicinity to form Al−O−$Al(CH_3)$−O−Al (monomethylaluminum) and $AlCH_3$ species.

As a TMA-analogous reaction, McFarlane et al. performed an infrared study on trimethylgallium (TMG) adsorbed on alumina, and found that TMG reacts with Al−OH groups on alumina to yield $AlOGa(CH_3)_2$ and CH_4 as TMA does in eq 2a.[21] In addition, they observed the Al−CH_3 surface species, which are bonded to the Lewis acidic Al atoms by the reaction of TMG with Lewis acid/base sites of alumina. Furthermore, Vandalon et al. have recently observed the presence of the persistent $AlCH_3$ groups, which are no longer reactive toward water during Al_2O_3 ALD at temperatures below ~200 °C.[8,22] According to their infrared studies using the technique of broadband sum-frequency generation, the persistent $AlCH_3$ groups are not incorporated into the film as a contaminant species. As is well known, the Al_2O_3 films grown by ALD using TMA and water are almost carbon-free.[23]

On the other hand, in several infrared studies of Al_2O_3 ALD using TMA and ozone (O_3),[24−26] formate (and/or carbonate) surface species were found to be an intermediate formed during exposing ozone onto the surface previously methylated by exposure to TMA. Therefore, we expect that ozone can be utilized as a chemical probe to detect the presence of the water-stable (persistent) $AlCH_3$ species on the growing surface by the ALD process, owing to its higher reactivity than water. Here, we provide an in-situ infrared study of Al_2O_3 ALD and report the chemical probing of the water-stable $AlCH_3$ surface species, which exists over the surface of alumina during Al_2O_3 ALD using TMA and water.

EXPERIMENTAL SECTION

In situ FTIR spectroscopic analyses were performed on silica pellets to understand the surface chemistry of Al_2O_3 ALD using various sequential exposures of TMA, H_2O (or D_2O), and ozone. As can be seen from the schematic diagram (Figure S1) of the in situ FTIR setup for transmission geometry, the infrared beam from a Nicolet iS50 FTIR spectrometer (Thermo Fisher Scientific, Inc.) was aligned through a ZnSe window to the silica pellet, which is placed vertically by a stainless-steel grid on the stage heater of an ALD reactor. A mercury cadmium telluride (MCT) detector cooled with liquid nitrogen was able to measure the IR spectra from 400 to 4000 cm^{-1} with a resolution of 4 cm^{-1}. During exposure to a precursor, the gate valves between ZnSe windows and the reactor were closed to prevent deposition on the ZnSe windows. All FTIR spectra were obtained by averaging 400 scans and were referenced to the ZnSe window as a background. Most FTIR spectra in this work are presented as difference spectra, which are referenced to the spectrum of the previous exposure.

The reactor was a warm-wall reactor capable of heating the chamber wall to 160 °C. Because the silica pellet in the stainless-steel grid was heated by the stage heater through a metal holder, the maximum temperature of the silica pellet monitored using a thermocouple was ~225 °C when the wall and stage were heated to 160 and 400 °C, respectively.

Fumed silica powder (S5505) was purchased from Sigma-Aldrich. The average diameter of the silica powder is 0.2−0.3 μm and the specific surface area is ~200 m^2/g (±25). To improve the signal-to-noise ratio of the FTIR spectra, the silica pellets were prepared to be porous by pressing the silica powder into a stainless-steel grid (0.1 mm thick; diameter 40 mm) with a mesh size of 0.4 mm. The preparation procedure for the silica pellets is as follows. A blank grid is put on a polypropylene (PP) film (diameter 40 mm, SpecroPellet Cat. no. 7040, Chemplex Industries, Inc.) placed on the lower anvil. Then, after spreading the silica powder (50 mg) evenly over the grid, another PP film is placed on it. After placing the upper anvil (diameter 40 mm) on the PP film, the pellet die assembly is placed into a hydraulic press and applied with a weight of ~5000 kgf. Upon removal of the grid from the anvils, there are slabs of silica powder stacked inside each hole of the grid. The silica powder pressed into the holes of the grid is firmly fixed to withstand soft bending.

TMA and D_2O were purchased from iChems Co., Ltd. (99.999%) and Sigma-Aldrich (99.994%), respectively. Water was deionized to ~18 MΩ·cm, and ozone was produced from oxygen gas (99.999%) using an ozone generator (OzoneTech). The ozone concentration was ~180 g/m^3 (~730 sccm of the total flow rate of ozone and oxygen gases with an ozone to oxygen ratio of 1/10) at the outlet of the ozone generator. High-purity nitrogen gas (99.999%) was used as a purging gas with a flow rate of 400 sccm. TMA and water (or D_2O) were stored at room temperature and delivered to the reactor without any carrier gas. The exposure times of precursors were controlled by pneumatic valves and their delivery lines were maintained to be 100 °C.

https://doi.org/10.1021/acs.jpcc.1c05889
J. Phys. Chem. C 2021, 125, 21434−21442

For exposures to liquid precursors [i.e., TMA and water (or D_2O)], the liquid precursor was fed into the reactor with a closed roughing valve until the reactor pressure reached ~10 torr and then held for 10 min. For exposure to ozone, ozone was fed for 10 min while pumping the reactor, and the reactor pressure reached ~1.7 Torr by the ozone supply. The detailed experimental conditions for FTIR measurements are listed in Table S1 (the on/off status of valves, reactor pressures, exposure times, and volumetric flow rates of each precursor). Except for the in situ FTIR experiments in Figures 3 and 4, the other FTIR experiments were performed on silica pellets on which the Al_2O_3 ALD process using TMA and water (or D_2O) was cycled 20 times to prepare the alumina surface on the silica. The processing time for each step was TMA (1 s), purge (30 s), water (2 s), and purge (30 s).

RESULTS AND DISCUSSION

Our experimental setup employed for the in-situ FTIR analysis is validated by a preliminary analysis for the typical sequence of Al_2O_3 ALD. As explained in the Experimental section, the FTIR absorbance was measured after purging the chamber to protect IR windows of ZnSe. Because the silica pellet strongly absorbs IR below 1250 cm^{-1} (see Figure S2), the IR spectra in the low-frequency range below 1300 cm^{-1} are noisy and not shown for clarity. Consequently, the symmetric $AlCH_3$ deformation mode expected to appear at 1211−1240 cm^{-1} has unfortunately not been resolved. Thus, we pay attention to the stretching vibrational modes of $AlCH_3$ in a high-frequency region of 2800−3000 cm^{-1}.[24−27]

Figure 1a shows difference spectra of in-situ FTIR in the sequence of Al_2O_3 ALD at 150 °C using TMA and water.

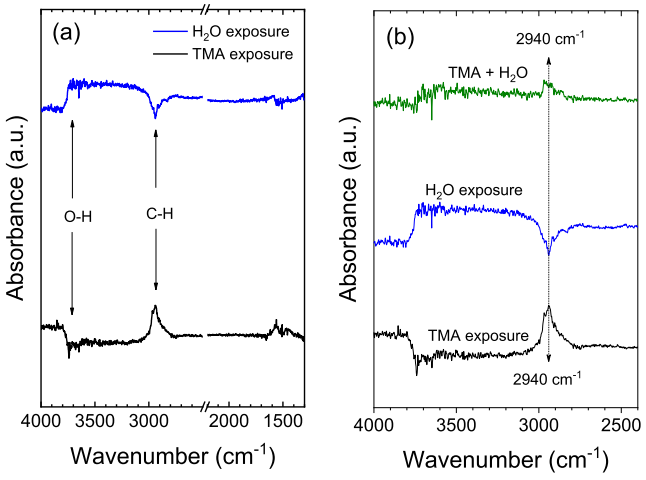

Figure 1. Difference FTIR spectra (a) of Al_2O_3 ALD at 150 °C using TMA and water. The right panel (b) shows the magnified spectra (black and blue) of (1a) and a sum spectrum (green), which was obtained by taking the sum of the other two difference spectra.

These difference spectra are referenced to the previous precursor exposure and are displaced from the origin for clarity. To prepare a starting Al_2O_3 surface on a silica pellet, Al_2O_3 ALD using TMA and water was performed for 20 cycles. Subsequently, TMA was exposed onto the surface, which was last exposed to water in the previous step. In Figure 1a (black line), vibrational features centered at 2940 cm^{-1} are assigned to the C−H stretching vibrations of $AlCH_3$ species formed by the TMA exposure.[24−27] On the other hand, the negative vibrational feature between ~3500 and 3800 cm^{-1} is assigned to the O−H stretching vibrations of AlOH species, which is consumed by the TMA exposure.[24−27] After water exposure (blue spectrum in Figure 1a), the positive vibrational feature of $AlCH_3$ and the negative vibrational feature of AlOH are converted to negative and positive features, respectively, owing to surface hydroxylation by the exposure to water (i.e., consumption of methyl groups and generation of hydroxyl groups). However, as shown in Figure 1b, the intensity of the positive features (black line) of the methyl stretching modes formed by the TMA exposure is not equal to that of the negative features (blue line) consumed by the water exposure. In other words, the surface methyl species do not completely react toward the water to form the surface hydroxyl groups. The presence of the persistent $AlCH_3$ may lead to this incomplete consumption of methyl groups. The contribution of the persistent methyl groups can be visualized in a sum spectrum (green) of Figure 1b, which was obtained by taking the sum of the other two difference spectra. The vertical-dotted arrow indicates the wavenumber of the peak at 2940 cm^{-1} as a guide to the eye. In the sum spectrum, a positive vibrational feature in the methyl stretching region represents the presence of the persistent methyl groups, which remained after undergoing the exposures included in the sum spectrum. In addition, the positive broad feature of hydroxyl groups in the sum spectrum reveals that the number of hydroxyl groups produced by water exposure is greater compared to the number of hydroxyls consumed by TMA adsorption. This indicates that the presence of the persistent methyls is not due to insufficient exposure to water. The concern about insufficient exposure to water will be discussed in detail in Figures 7 and S8. As a result, the sum spectrum exhibits some methyl groups remain with hydroxyl groups after the sequential exposures of TMA and water.

Figure 2a shows the difference spectra in the sequence of Al_2O_3 ALD at 150 °C using TMA and ozone. The in situ difference spectra were obtained after performing 20 cycles of Al_2O_3 ALD. By the sequential exposures of TMA (black spectrum) and ozone (red spectrum), the positive vibrational feature of $AlCH_3$ centered at 2940 cm^{-1} is converted to the

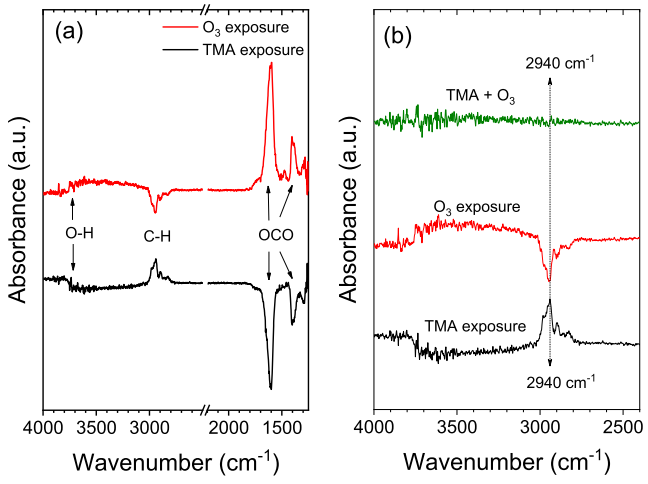

Figure 2. Difference FTIR spectra (a) of Al_2O_3 ALD at 150 °C using TMA and ozone. The right panel (b) shows the magnified spectra (black and red) of (2a) and a sum spectrum (green), which was obtained by taking the sum of the other two difference spectra.

https://doi.org/10.1021/acs.jpcc.1c05889
J. Phys. Chem. C 2021, 125, 21434−21442

negative feature because the $AlCH_3$ species are consumed by ozone exposure.[24−26] The negative O−H stretching feature consumed by TMA exposure is also converted to a positive absorbance by ozone exposure because AlOH species are regenerated via a formate intermediate as previously reported.[24−26] The characteristic strong mode of the asymmetric OCO stretching vibrations of formate species is resolved at 1596 cm^{-1}, which becomes negative by the TMA exposure and positive by the ozone exposure. The absorption features at ∼1404 cm^{-1} correspond to the overlapped modes of symmetric OCO stretching and C−H in-plane bending vibrations of the formate.[28−30] These observed vibration modes of the formate species formed by the TMA/ozone process are listed in Table 1 (second column), and are compared to the literature values.[24,25]

Table 1. Band Assignments of Observed Vibrational Frequencies (cm^{-1}) for the Surface Formate Formed by Ozone Exposure and Their Comparison with Literature Values

	this work			ref 25	
mode	TMA/O_3 (Figure 2a)	$TMA/H_2O/O_3$ (Figure 3a)	Ref 24	obs.	cal.
ν_s (OCO)	1383[a]	1385[a]	1388	1360	1350
δ (CH)	1404[a]	1404[a]	1404	1385	1393
ν_{as} (OCO)	1596	1609	1597	1610	1622

[a]These values are not resolved due to the overlap of ν_s (OCO) and δ (CH) modes of formate species. Thus, the peak positions of ν_s (OCO) were determined from the shoulder of δ (CH).

In Figure 2b, the intensity of the positive features of the methyl stretching modes formed by the TMA exposure is almost equal to the intensity of the negative features consumed by the ozone exposure. This reveals that the surface methyl species are almost completely consumed to form other surface species including the formate species. Consequently, the featureless spectral line in the methyl stretching region of the sum spectrum (green spectrum in Figure 2b) indicates that the $AlCH_3$ species are not stable to ozone. In addition, the noisy spectral line in the hydroxyl stretching region shows that the number of hydroxyl groups produced by ozone exposure is approximately equal to that of hydroxyls consumed by TMA exposure.

To investigate whether ozone could be used as a chemical probe for the persistent $SiCH_3$ groups, a series of sequential exposures consisting of TMA, water, and ozone were performed onto a bare silica pellet (no ALD cycle before this experiment). For each exposure, difference spectra, referenced to the spectrum of the previous exposure, were obtained as shown in Figure 3. Each difference spectrum was plotted from bottom to top according to the exposure sequence. The difference spectra are represented by a combination of Roman letters (t: TMA, w: water, and o: ozone) and numbers. The characteristic vibrational modes of hydroxyls (O−H stretching), methyls, (C−H stretching), and formates (asymmetric OCO stretching) are eye-guided with vertical-dotted lines. The difference spectra in high frequency- and low-frequency regions are shown in Figure 3a,b, respectively.

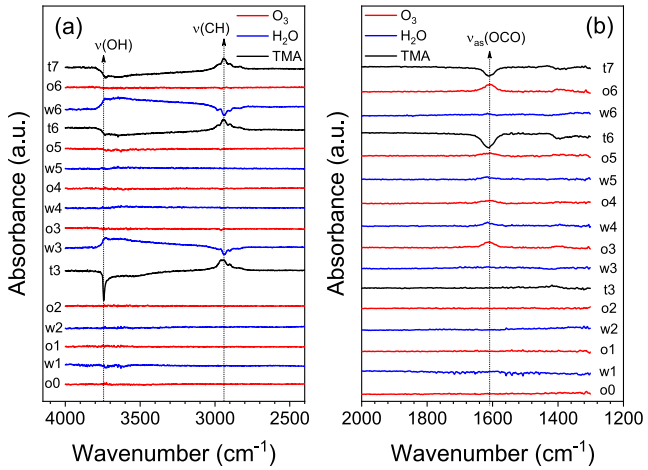

Figure 3. Difference FTIR spectra in a series of sequential exposures consisting of TMA, water, and ozone at 150 °C: (a) high-frequency spectra; (b) low-frequency spectra.

The bare silica pellet was first exposed to ozone and then sequential exposures of water and ozone were repeated twice to obtain a clean surface. During these exposures (from o0 to o2), there are no significant vibrational features in the high- and low-frequency regions. After the first TMA exposure (t3), a sharp negative feature of the isolated O−H stretching mode is observed at 3744 cm^{-1} with a broad negative shoulder of hydrogen-bonded OH stretching vibrations.[24−27,31] Note that the bare silica pellet shows a sharp peak at ∼3744 cm^{-1} in Figure S2, indicating the presence of the isolated OH groups on the surface. The sharp negative peak at 3744 cm^{-1} in Figure 3a (t3) is attributed to the consumption of the isolated OH groups by TMA adsorption. The C−H stretching vibrations of methyl species are also observed at ∼2940 cm^{-1} with a positive feature due to the chemisorption of TMA. In the next exposure to water (w3), the negative O−H and positive C−H stretching modes are converted to positive and negative features, respectively, owing to hydroxylation by the ligand exchange reaction (eq 2b). The vibrational characteristics of the spectra t3 and w3 are similar to those of Figure 1a.

In the next ozone exposure (o3) onto the surface, which is expected to be already hydroxylated in the previous exposure to water (w3), the asymmetric OCO stretching vibration of formate species is positively resolved at ∼1609 cm^{-1}. The overlapped band of the symmetric OCO stretching and C−H in-plane bending vibrations of formate species are also visible at ∼1404 cm^{-1} (see Figure S3 for magnified spectra). This observation is surprising because the formate species cannot be formed without surface species containing carbon. Therefore, it reveals that carbon-containing species (i.e., persistent methyl groups) had been present on the hydroxylated surface before the exposure to ozone (o3) and are chemically probed by the exposure to ozone.

Figure 4a shows the magnified difference spectra of exposures of t3 to o3. The positive features of the methyl groups formed by the TMA exposure (t3) are more intense than those of the negative features by the water exposure (w3). This indicates that the water-stable (persistent) methyl groups are remaining on the surface even though the hydroxylated surface has been formed by exposure to water. The presence of the persistent methyl groups is visible as a peak centered at ∼2960 cm^{-1} in the sum spectrum (green), which is obtained

https://doi.org/10.1021/acs.jpcc.1c05889
J. Phys. Chem. C 2021, 125, 21434−21442

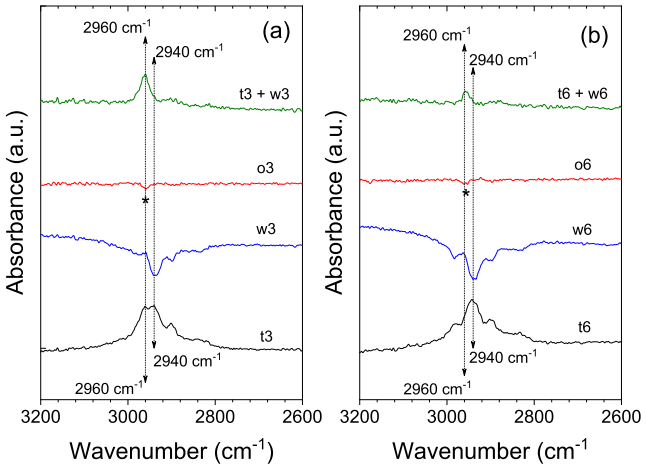

Figure 4. Magnified difference FTIR spectra selected from Figure 3: (a) t3 to o3; (b) t6 to o6. The sum spectra (green) were obtained by taking the sum of the other two difference spectra [t3 + w3 (a); t6 + w6 (b)].

by taking the sum of spectra t3 and w3 (see Figure S4a for the sum spectrum including the OH stretching region). This persistent methyl species may be bonded to Si atoms of silica as previously assigned by several groups.[6,16−19] Note that there is a small negative feature (denoted with an asterisk) in the difference spectrum of o3 (Figure 4a). This peak is indeed observed at the same wavenumber of ∼2960 cm^{-1} as in the sum spectrum (t3 + w3) because the persistent methyl species are consumed to form the formate species by the ozone reaction. However, the negative feature of the difference spectrum (o3) is smaller than the positive feature of the sum spectrum (t3 + w3). This reveals that the water-stable $SiCH_3$ species are not completely consumed but partially remained even after the ozone exposure.

In Figures 3b and S3, during the subsequent exposures to water and ozone from w4 to o5, there is a weak and broad feature at ∼1609 cm^{-1}. The peak at ∼1609 cm^{-1} does not show any negative features but rather slightly positive features during the exposures of o3 to o5. It indicates that the $SiCH_3$ species are continuously converted to the formate species during the exposures of o3 to o5. Consequently, the population of the surface formate species after the ozone exposure of o5 is expected to be more abundant than the population after the ozone exposure of o3.

In the second TMA exposure (t6) of Figure 3a, the vibrational modes of methyl groups again appear positively at ∼2940 cm^{-1} and the OH stretching mode shows negative features. Because the surface hydroxyls formed by the water exposure of w3 do not disappear in the sequential exposures from o3 to o5, TMA molecules are chemically adsorbed via the ligand exchange reaction to form the methyl species as in the ALD process using TMA and ozone (Figure 2). Moreover, because the surface before the second TMA exposure (t6) has not only hydroxyls but also formate species formed in the sequential exposures from o3 to o5 (Figure 3b), prominent vibrational features of formate species are again observed negatively at ∼1609 and ∼1404 cm^{-1} (see Figure S3 for the magnified spectrum of t6). This indicates the consumption of the formate species by an unknown reaction between formate surface species and TMA. Furthermore, as shown in Figure S3, the sum spectrum of o3 to t6 is a noisy horizontal line and has no significant vibrational feature. It reveals that the formate species formed by the exposures of o3 to o5 are almost converted to other surface species without vibrational mode in this range and the newly formed species have methyl groups as seen in the spectrum t6 of Figure 3a (see Scheme 2 and its explanation for the identity of the newly formed species).

Scheme 2. Proposed Reaction Between Surface Formate Species and TMA

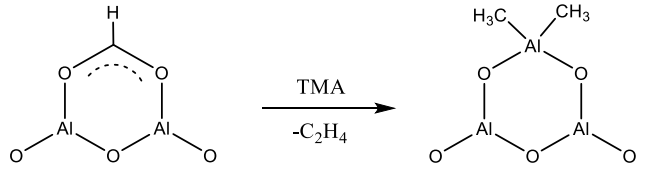

bridging formate (type II)

In the next water exposure of w6 in Figure 3a, the surface is rehydroxylated, and the surface methyl groups again disappear as indicated by the positive OH stretching and negative C−H stretching modes, respectively. However, there is no significant vibrational feature in the low-frequency region (Figure 3b). Figure 4b shows the magnified difference spectra of the exposures of t6 (black) and w6 (blue). The positive intensity of t6 is slightly higher than the negative intensity of w6. Thus, the sum spectrum (green) of t6 + w6 is much weaker than that of t3 + w3 in Figure 4 (see Figure S4b for the sum spectrum including the OH stretching region). This reveals that the number of the water-stable methyl species formed by the second TMA exposure (t6) is much smaller than that by the first TMA exposure (t3). It is believed that the water-stable methyl species are mainly $SiCH_3$ in the first TMA exposure and a mixture of $SiCH_3$ and $AlCH_3$ in the second TMA exposure because at least 5 or more ALD cycles are required to form a full Al_2O_3 layer on a bare silica pellet as reported by Levrau and co-workers.[16]

In the next ozone exposure of o6, the positive features of formate species reappear upon exposure to ozone (Figure 3b), and there is also a small negative feature (denoted with an asterisk in Figure 4b) indicating the disappearance of methyl species. It reveals that the water-stable methyl groups ($AlCH_3$ and $SiCH_3$) are converted to the formate species upon exposure to ozone. In the subsequent third TMA exposure of t7 (Figure 3), the vibrational features in the high- and low-frequency regions are again similar to those of the second TMA exposure of t6. However, because ozone (o6) was exposed only once after the second TMA exposure (t6), the formate species formed by the ozone exposure (o6) almost disappear upon exposure to TMA (t7) as revealed in Figure S5 (sum spectrum of o6 + t7).

Another concern for the ozone exposure steps of o3 and o6 is that there is no significant variation in the O−H stretching features in the high-frequency region (Figure 3a). This indicates that the hydroxyl species previously formed in the water exposure steps of w3 and w6 are not significantly affected by the ozone exposure. Consequently, the surface hydroxyl species also serve as adsorption sites in the subsequent exposure to TMA.

According to the in-situ FTIR analysis in Figure 3, the vibrational characteristics of the surface formate are summarized as follows: (1) the vibrational modes of formate are at least not attenuated by exposure to ozone (see spectra o3 to o5 in Figure 3b). (2) The TMA exposure onto the

https://doi.org/10.1021/acs.jpcc.1c05889
J. Phys. Chem. C 2021, 125, 21434−21442

surface containing formate species converts the positive vibrational modes of formates into the negative features of nearly equal intensity. Given these characteristics, the mechanism of ozone reaction proposed in the previous studies of Al_2O_3 ALD using TMA and ozone, where the formate is an unstable intermediate, is questionable.[24,25] As is well known, ALD using TMA and ozone grows almost carbon-free Al_2O_3 films.[24,25,32] Therefore, the surface formate species must disappear upon exposure to TMA to leave no carbon impurities. However, if the only pathway for the disappearance of the formate species is thermal decomposition liberating CO or CO_2 as in their mechanism, the conversion of the positive vibrational features of formate to the negative features by the TMA exposure is not clearly explained. Moreover, because the formate species are not vulnerable to ozone, it is believed that the formate species are not an unstable intermediate, but a rather stable surface species, which coexists with hydroxyl groups on the surface exposed to ozone.

We propose in Scheme 2, a plausible reaction between the surface formate and TMA. It is well known that there are several types of surface formate species such as monodentate (type I), bridging (type II), and bidentate (type III) formate ions.[33−35] An empirical approach using ν(OCO) modes to identify the coordination type of formate species has been proposed by Busca and Lorenzelli.[33] The difference between the asymmetric and the symmetric OCO stretching modes, $\Delta\nu = \nu_{as}$ (OCO) − ν_s (OCO), in the low-frequency region depends on the coordination type of formates. According to the coordination type, the $\Delta\nu$ values are arranged in the following order of magnitude: type I (monodentate) > type III (bridging) ≥ type II (bidentate).[33−35] Considering the values of $\Delta\nu$ (210−220 cm^{-1}), the major configuration of formate species is the bridging structure (type II), which is the most stable configuration of formate species.[35] In Scheme 2, because Al atoms prefer a tetra-coordinated surface complex, the central Al of TMA may react with two oxygen atoms of formate to form DMA surface species liberating ethylene (C_2H_4). Consequently, upon exposure to TMA, the positive vibrational features of formate are converted to the negative features, and the surface is again terminated with methyl groups. The reaction of Scheme 2 may be applied to the TMA/ozone process (Figure 2) as well as the TMA/water/ozone process (Figure 3) because the formate species disappear by the TMA exposure in both processes. The reaction between the surface formate species and TMA in Scheme 2 is also supported by the previous in-situ FTIR analysis by Goldstein and coworkers.[24] In their work (Figure 4 of ref 24), the formate species were formed by exposing Al_2O_3 to formaldehyde. The characteristic peaks of OCO were observed positively upon exposure to formaldehyde and negatively upon subsequent exposure to TMA. In addition, the methyl stretching modes formed by the TMA adsorption were also positively observed at 2920−2980 cm^{-1} upon exposure to TMA. This indicates that the surface formate species react with TMA to consume the formate species, and the formate consumption leaves methyl groups on the surface.

To investigate the temperature dependency of chemical probing by ozone (Figure 5), we performed a series of sequential exposures consisting of TMA, D_2O, and ozone in the temperature range of 150−225 °C onto a silica pellet. Al_2O_3 ALD using TMA and D_2O was first performed on the silica pellet at 225 °C for 20 cycles. Subsequently, TMA, D_2O, and ozone were sequentially exposed at the same temperature,

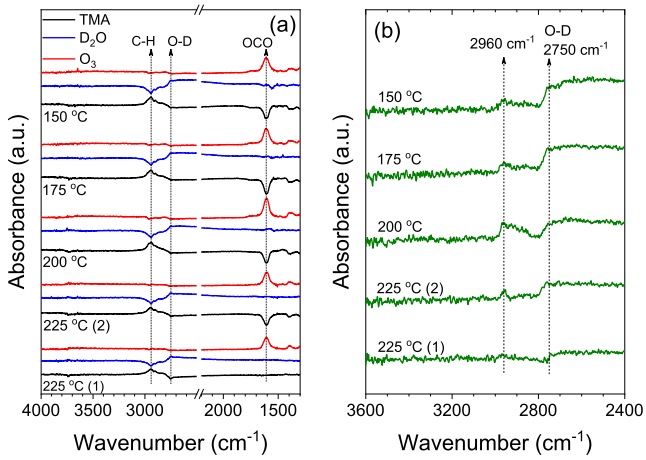

Figure 5. (a) Difference FTIR spectra in a series of sequential exposures consisting of TMA, D_2O, and ozone in the temperature range of 150−225 °C; (b) sum spectra at each temperature obtained by taking the sum of the difference spectra of the TMA exposure and D_2O exposure at each temperature.

and difference FTIR spectra were obtained for each exposure after purging the chamber. Similar experiments were repeated while lowing the temperature by 25 to 150 °C. The sequential exposures were repeated twice at 225 °C to observe the formate peaks and once at the other temperatures.

In Figure 5a (black spectra), upon exposure to TMA, the vibrational features of methyl species are observed positively at ∼2940 cm^{-1}, and the stretching vibrational modes of deuteroxyl (OD) species appear negatively near 2750 cm^{-1} for all temperatures.[6] This is due to the chemisorption of TMA, which consumes the deuteroxyl species. The vibrational features of formate species are also observed negatively at ∼1609 cm^{-1} for all temperatures, but not visible in the spectrum of the first TMA exposure at 225 °C. Note that the previous steps of the TMA exposures are the ozone exposures except for the first TMA exposure at 225 °C. Therefore, this reveals that there are two kinds of adsorption sites, that is, deuteroxyls and formates species, on the surface formed when exposed to ozone. For the first TMA exposure at 225 °C, the previous step is the D_2O exposure in the 20th cycle of Al_2O_3 ALD, thus there are only deuteroxyls as the adsorption sites and no formate species produced by the ozone reaction with the persistent methyl species.

Upon exposure to D_2O (blue spectra in Figure 5a), the vibrational features of methyl species are converted to negative bands at ∼2940 cm^{-1}, and the stretching vibrational modes of deuteroxyl species are observed positively near 2750 cm^{-1} for all temperatures. This is attributed to the deuteroxylation of surface methyl species. After the deuteroxylation, the presence of water-stable (persistent) $AlCH_3$ species is confirmed in the sum spectra (Figure 5b) obtained by taking the sum of the difference spectra in the TMA exposure and D_2O exposure steps. Regardless of the temperature, the vibrational modes of the water-stable methyl species appear at ∼2960 cm^{-1}, but their intensities are temperature-dependent.

Upon exposure to ozone (red spectra in Figure 5a), the most prominent feature of the asymmetric stretching of OCO appears positively at ∼1609 cm^{-1} at all temperatures (Figures 5a and 6b). In addition, a small vibrational feature of the water-stable (persistent) $AlCH_3$ species is observed negatively at ∼2960−2965 cm^{-1} as clearly shown in the magnified

https://doi.org/10.1021/acs.jpcc.1c05889
J. Phys. Chem. C 2021, 125, 21434−21442

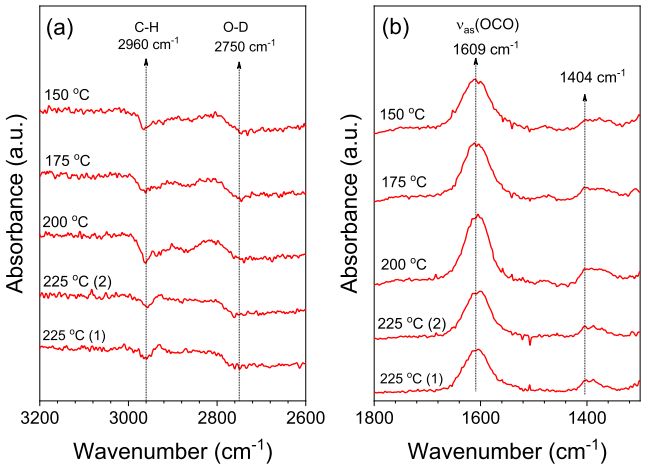

Figure 6. Magnified difference FTIR spectra of the ozone exposure steps selected from Figure 5: (a) high-frequency spectra; (b) low-frequency spectra.

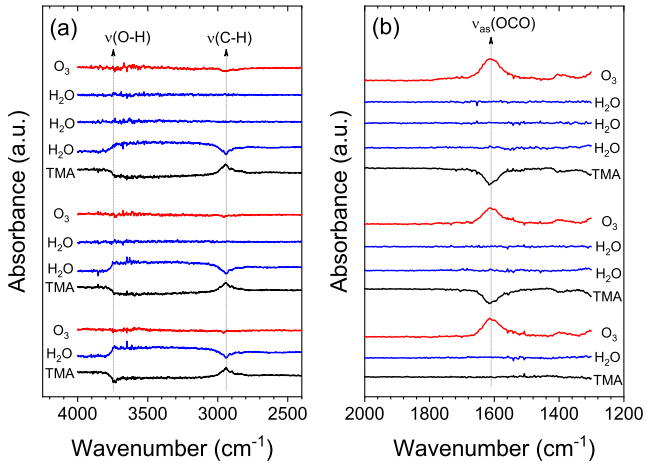

Figure 7. Difference FTIR spectra according to the number of water exposures between exposures of TMA and ozone at 150 °C: (a) high-frequency spectra; (b) low-frequency spectra.

difference spectra of Figure 6a. The peak position is close to that (2958−2960 cm^{-1}) of the persistent methyl groups in previous reports.[6,18,36] In Figure 6a,b, both intensities of the negative peaks of the persistent $AlCH_3$ and the positive peaks of the OCO species increase from 150 to 200 °C and decrease at 225 °C. The highest peak of the ν_{as} (OCO) mode is observed at 200 °C with a full width at half-maximum (fwhm) of 56 cm^{-1} (see Figure S6 for the normalized intensities and fwhms at various temperatures). Moreover, the water-stable $AlCH_3$ species almost disappears at all temperatures when exposed to ozone as revealed with noisy horizontal lines in the sum spectra (Figure S7), which were obtained by taking the sum of three difference spectra of TMA, D_2O, and ozone exposures at each temperature. This indicates that the water-stable $AlCH_3$ species are chemically probed by the ozone reaction.

To address a remained concern that insufficient exposure to water could result in the persistent methyl species, we investigated whether the number of water exposures between exposures of TMA and ozone affected the formation of the surface formate species. A series of sequential exposures consisting of TMA, water, and ozone were performed on a silica pellet (20-cycled for Al_2O_3 ALD using TMA and water) to obtain difference spectra of each exposure (Figure 7). As clearly seen in Figure 7b, when the hydroxylated surface is exposed to ozone, the prominent vibrational features of OCO are observed at ∼1609 cm^{-1}, regardless of the number of water exposures. This shows that the water-stable (persistent) $AlCH_3$ species have extremely low reactivity toward the water and are not formed due to insufficient exposure to water. Indeed, when the exposure to water is insufficient, the positive methyl stretching modes were not fully converted to the negative peaks upon exposure to water (see Figure S8). That is why we fed water into the reactor with a closed roughing valve until the reactor pressure reached ∼10 torr and then held for 10 min as listed in Table S1.

According to the IR study on the reaction between TMA and water on the surface of alumina by Soto and Tysoe,[36] there are two types of $AlCH_3$ surface species: one reacts rapidly with water and the other reacts approximately 30 times more slowly. The water-stable (persistent) methyl groups, of which the C−H stretching mode is assigned to ∼2960 cm^{-1} in this work, may be bound to Al atoms in the lattice of alumina via Lewis acid−base interaction, rather than the Al atoms belonging to the overlayer of adsorbates (Scheme 1).[37,38] It is inferred that the temperature dependency of the persistent methyl groups observed in Figures 5 and 6 may be related to the methyl transfer reaction of Scheme 1. As aforementioned in the introduction section, the methyl transfer reaction occurs on a hydroxylated surface with a low OH coverage.[20] The methyl transfer can be more activated to form the persistent methyl species at higher temperatures because the number of the bridged oxygens (Al−O−Al) increases with temperature by dehydroxylation. However, because the water stability of the persistent methyls is attenuated by activation of hydroxylation at higher temperatures, the persistent methyl groups may show the temperature dependency of rise and fall.

Recently, Lownsbury et al. reported in situ calorimetric measurement of the heat of adsorption for two half-reactions of Al_2O_3 ALD using TMA and water.[39] The quantified exothermic heat of adsorption is −343 kJ/mol TMA for the TMA half-reaction (eq 2a) and −251 kJ/mol H_2O for the water half-reaction (eq 2b). It was observed that, which is more interesting to us, there is a distinct difference in the heat signal after saturation between the TMA pulse and the water pulse. For TMA pulses, their heat signal at saturation is only ∼1% of the intensity of the first TMA pulse. Unlike the TMA pulses, even at saturation, the heat signal of the water pulse is ∼25% as intense as the first water pulse. The authors attribute the significantly large heat signal observed after saturation to reversible adsorption and desorption of water. However, we believe that the remaining heat signal is attributed to the persistent methyl species.

CONCLUSIONS

The surface reactions of Al_2O_3 ALD were investigated by in situ FTIR spectroscopy focusing on the presence of water-stable (persistent) methyl species. The existence of the persistent methyl groups was confirmed in Al_2O_3 ALD using TMA and water and chemically probed by the ozone reaction in which formate species were formed from the persistent methyl groups. The water-stable methyl species were observed in the temperature range of 150−225 °C. Up to 200 °C, the higher temperature, the stronger the vibrational bands of the persistent methyl groups and formate species. However, both

https://doi.org/10.1021/acs.jpcc.1c05889
J. Phys. Chem. C 2021, 125, 21434−21442

intensities are lowered at 225 °C. Therefore, it is expected that the presence and the amount of the persistent methyl groups are temperature-dependent.

A plausible reaction between surface formate species and TMA was also proposed based on the in situ FTIR analysis. Considering the stability of the formate species when exposed to ozone, it is believed that the formate species serve as adsorption sites for TMA in Al_2O_3 ALD using TMA and ozone, but not as an intermediate species.

■ ASSOCIATED CONTENT

Supporting Information

The Supporting Information is available free of charge at https://pubs.acs.org/doi/10.1021/acs.jpcc.1c05889.

Schematic diagram of the experimental setup; experimental conditions for FTIR measurements; FTIR spectrum of bare silica pellets; magnified difference spectra selected from Figures 3 and 5; and normalized intensities and fwhms of the asymmetric OCO stretching mode at various temperatures (PDF)

■ AUTHOR INFORMATION

Corresponding Author

Yo-Sep Min − *Department of Chemical Engineering, Konkuk University, Seoul 05029, Korea;* orcid.org/0000-0002-2340-3633; Email: ysmin@konkuk.ac.kr

Authors

Zhenyu Jin − *Department of Chemical Engineering, Konkuk University, Seoul 05029, Korea*

Suhyun Lee − *Department of Chemical Engineering, Konkuk University, Seoul 05029, Korea*

Seokhee Shin − *Department of Chemical Engineering, Konkuk University, Seoul 05029, Korea*

Da-Som Shin − *Department of Chemical Engineering, Konkuk University, Seoul 05029, Korea*

Hyeri Choi − *Department of Chemical Engineering, Konkuk University, Seoul 05029, Korea*

Complete contact information is available at: https://pubs.acs.org/10.1021/acs.jpcc.1c05889

Notes

The authors declare no competing financial interest.

■ ACKNOWLEDGMENTS

This work was supported by the Samsung Research Funding & Incubation Center of Samsung Electronics (SFRC-MA1801-01). This work was also partially supported by Basic Science Research Program through the National Research Foundation of Korea (NRF: 2021R1F1A1059930), which is funded by the Ministry of Education. This paper was also supported by the Konkuk University in 2019.

■ REFERENCES

(1) George, S. M. Atomic layer deposition: an overview. *Chem. Rev.* **2010**, *110*, 111−131.

(2) Hwang, C. S. *Atomic Layer Deposition for Semiconductors*; Springer: New York, NY, 2014.

(3) Puurunen, R. L. Surface chemistry of atomic layer deposition: a case study for the trimethylaluminum/water process. *J. Appl. Phys.* **2005**, *97*, 121301.

(4) Juppo, M.; Rahtu, A.; Ritala, M.; Leskelä, M. In situ mass spectrometry study on surface reactions in atomic layer deposition of Al_2O_3 thin films from trimethylaluminum and water. *Langmuir* **2000**, *16*, 4034−4039.

(5) Rahtu, A.; Alaranta, T.; Ritala, M. In situ quartz crystal microbalance and quadrupole mass spectrometry studies of atomic layer deposition of aluminum oxide from trimethylaluminum and water. *Langmuir* **2001**, *17*, 6506−6509.

(6) Frank, M. M.; Chabal, Y. J.; Wilk, G. D. Nucleation and interface formation mechanisms in atomic layer deposition of gate oxides. *Appl. Phys. Lett.* **2003**, *82*, 4758−4760.

(7) Wind, R. A.; George, S. M. Quartz crystal microbalance studies of Al_2O_3 atomic layer deposition using trimethylaluminum and water at 125 °C. *J. Phys. Chem. A* **2010**, *114*, 1281−1289.

(8) Vandalon, V.; Kessels, W. M. M. Revisiting the growth mechanism of atomic layer deposition of Al2O3: a vibrational sum-frequency generation study. *J. Vac. Sci. Technol., A* **2017**, *35*, 05C313.

(9) Widjaja, Y.; Musgrave, C. B. Quantum chemical study of the mechanism of aluminum oxide atomic layer deposition. *Appl. Phys. Lett.* **2002**, *80*, 3304−3306.

(10) Elliott, S. D. Predictive process design: a theoretical model of atomic layer deposition. *Comput. Mater. Sci.* **2005**, *33*, 20−25.

(11) Ghosh, M. K.; Choi, C. H. The initial mechanisms of Al_2O_3 atomic layer deposition on OH/Si(100)-2×1 surface by trimethylaluminum and water. *Chem. Phys. Lett.* **2006**, *426*, 365−369.

(12) Hu, Z.; Turner, C. H. Oxygen incorporation mechanism during atomic layer deposition of Al2O3 onto H-passivated Si(100)-2×1. *J. Phys. Chem. C* **2007**, *111*, 5756−5759.

(13) Weckman, T.; Laasonen, K. First principles study of the atomic layer deposition of alumina by TMA-H_2O-process. *Phys. Chem. Chem. Phys.* **2015**, *17*, 17322−17334.

(14) Seo, S.; Nam, T.; Lee, H.-B. -R.; Kim, H.; Shong, B. Molecular oxidation of surface -CH_3 during atomic layer deposition of Al_2O_3 with H_2O, H_2O_2, and O_3: a theoretical study. *Appl. Surf. Sci.* **2018**, *457*, 376−380.

(15) Choi, J. W.; Ham, S.-Y.; Lee, S.; Shin, D.-S.; Min, Y.-S.; Kim, K. C. Unveiled understanding on thermodynamic mechanisms of atomic layer deposition based on trimethylaluminum and water precursors. *Ind. Eng. Chem. Res.* **2020**, *59*, 13325−13332.

(16) Levrau, E.; Van de Kerckhove, K.; Devloo-Casier, K.; Sree, S. P.; Martens, J. A.; Detavernier, C.; Dendooven, J. In-situ IR spectroscopic investigation of alumina ALD on porous silica films: thermal versus plasma-enhanced ALD. *J. Phys. Chem. C* **2014**, *118*, 29854−29859.

(17) Sandupatla, A. S.; Alexopoulos, K.; Reyniers, M.-F.; Marin, G. B. DFT investigation into alumina ALD growth inhibition on hydroxylated amorphous silica surface. *J. Phys. Chem. C* **2015**, *119*, 18380−18388.

(18) Yates, D. J. C.; Dembinski, G. W.; Kroll, W. R.; Elliott, J. J. Infrared studies of the reactions between silica and trimethylaluminum. *J. Phys. Chem.* **1969**, *73*, 911−921.

(19) Bartram, M. E.; Michalske, T. A.; Rogers, J. W., Jr. A reexamination of the chemisorption of trimethylaluminum on silica. *J. Phys. Chem.* **1991**, *95*, 4453−4463.

(20) Dillon, A. C.; Ott, A. W.; Way, J. D.; George, S. M. Surface chemistry of Al_2O_3 deposition using $Al(CH_3)_3$ and H_2O in a binary reaction sequence. *Surf. Sci.* **1995**, *322*, 230−242.

(21) McFarlane, R. A.; Morrow, B. A. An infrared study of trimethylgallium adsorbed on alumina and the Lewis/hydroxyl site ratio. *J. Phys. Chem.* **1988**, *92*, 5800−5803.

(22) Vandalon, V.; Kessels, W. M. M. What is limiting low-temperature atomic layer deposition of Al_2O_3? A vibrational sum-frequency generation study. *Appl. Phys. Lett.* **2016**, *108*, 011607.

(23) Guerra-Nuñez, C.; Döbeli, M.; Michler, J.; Utke, I. Reaction and growth mechanisms in Al_2O_3 deposited by atomic layer deposition: elucidating the hydrogen source. *Chem. Mater.* **2017**, *29*, 8690−8703.

(24) Goldstein, D. N.; McCormick, J. A.; George, S. M. Al_2O_3 atomic layer deposition with trimethylaluminum and ozone studied by in situ transmission FTIR spectroscopy and quadrupole mass spectrometry. *J. Phys. Chem. C* **2008**, *112*, 19530−19539.

(25) Kwon, J.; Dai, M.; Halls, M. D.; Chabal, Y. J. Detection of a formate surface intermediate in the atomic layer deposition of high-k dielectrics using ozone. *Chem. Mater.* **2008**, *20*, 3248−3250.
(26) Rai, V. R.; Vandalon, V.; Agarwal, S. Surface reaction mechanisms during ozone and oxygen plasma assisted atomic layer deposition of aluminum oxide. *Langmuir* **2010**, *26*, 13732−13735.
(27) Ferguson, J. D.; Weimer, A. W.; George, S. M. Atomic layer deprosition of ultrathin and conformal Al_2O_3 films on BN particles. *Thin Solid Films* **2000**, *371*, 95−104.
(28) Busca, G.; Lamotte, J.; Lavalley, J. C.; Lorenzelli, V. FT-IR study of the adsorption and transformation of formaldehyde on oxide surfaces. *J. Am. Chem. Soc.* **1987**, *109*, 5197−5202.
(29) Boiadjiev, V.; Tysoe, W. T. Infrared study of the surface species formed by sequential chemical vapor deposition of trimethylaluminum and methanol on a hydroxylated alumina surface. *Chem. Mater.* **1998**, *10*, 334−344.
(30) McInroy, A. R.; Lundie, D. T.; Winfield, J. M.; Dudman, C. C.; Jones, P.; Lennon, D. The application of diffuse reflectance infrared spectroscopy and temperature-programmed desorption to investigate the interaction of methanol on η-alumina. *Langmuir* **2005**, *21*, 11092−11098.
(31) Knözinger, H.; Ratnasamy, P. Catalytic aluminas: surface models and characterization of surface sites. *Catal. Rev. Sci. Eng.* **1978**, *17*, 31−70.
(32) Kim, S. K.; Lee, S. W.; Hwang, C. S.; Min, Y.-S.; Won, J. Y.; Jeong, J. Low temperature (<100 °C) deposition of aluminum oxide thin films by ALD with O_3 as oxidant. *J. Electrochem. Soc.* **2006**, *153*, F69−F76.
(33) Busca, G.; Lorenzelli, V. Infrared spectroscopic identification of species arising from reactive adsorption of carbon dioxides on metal oxide surfaces. *Mater. Chem.* **1982**, *7*, 89−126.
(34) Gopal, P.; Schneider, R. L.; Watters, K. L. Evidence for production of surface formate upon direct reaction of CO with alumina and magnesia. *J. Catal.* **1987**, *105*, 366−372.
(35) Calatayud, M.; Collins, S. E.; Baltanás, M. A.; Bonivardi, A. L. Stability of formate species on β-Ga_2O_3. *Phys. Chem. Chem. Phys.* **2009**, *11*, 1397−1405.
(36) Soto, C.; Tysoe, W. T. The reaction pathway for the growth of alumina on high surface area alumina and in ultrahigh vacuum by a reaction between trimethylaluminum and water. *J. Vac. Sci. Technol., A* **1991**, *9*, 2686−2695.
(37) Boiadjiev, V.; Tysoe, W. T. Infrared study of the surface species formed by sequential chemical vapor deposition of dimethylzinc and ethanthiol on hydroxylated alumina surfaces. *Chem. Mater.* **1998**, *10*, 1141−1152.
(38) Sandupatla, A. S.; Alexopoulos, K.; Reyniers, M.-F.; Marin, G. B. Ab initio investigation of surface chemistry of alumina ALD on hydroxylated γ-alumina surface. *J. Phys. Chem. C* **2015**, *119*, 13050−13061.
(39) Lownsbury, J. M.; Gladden, J. A.; Campbell, C. T.; Kim, I. S.; Martinson, A. B. F. Direct measurements of half-cycle reaction heats during atomic layer deposition by calorimetry. *Chem. Mater.* **2017**, *29*, 8566−8577.

https://doi.org/10.1021/acs.jpcc.1c05889
J. Phys. Chem. C 2021, 125, 21434−21442

Supporting Information

Chemical Probing of Water-Stable Methyl Species in Atomic Layer Deposition of Al_2O_3 from Trimethylaluminum and Water

Zhenyu Jin, Suhyun Lee, Seokhee Shin, Da-Som Shin, Hyeri Choi, and Yo-Sep Min*

Department of Chemical Engineering, Konkuk University, 120 Neungdong-Ro, Gwangjin-Gu, Seoul 05029, Korea

*Y. S. Min. Email: ysmin@konkuk.ac.kr

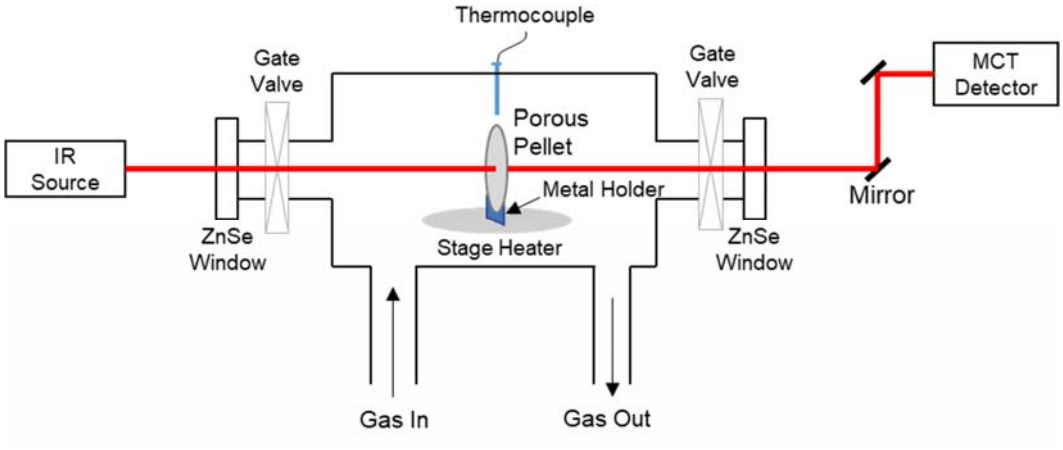

Figure S1. Schematic diagram of in-situ FTIR spectroscopic setup with transmission geometry. The silica pellet was prepared to be porous by pressing silica powder into a stainless-steel grid with 0.4 mm mesh.

Table S1. Experimental Conditions for FTIR Measurements in Exposure to Each Precursor

	Gate valves to ZnSe windows	Roughing valve to pump	Pressure (torr)	Time (min)	Flow rate (sccm)
TMA exposure	closed	closed	10	10	-
N_2 purging	closed	open	~2.2	3	400
IR measurement	open	open	< 0.05	~10[a]	-
Water exposure	closed	closed	10	10	-
N_2 purging	closed	open	~2.2	3	400
IR measurement	open	open	< 0.05	~10[a]	-
Ozone exposure	closed	open	1.7	10	~230
N_2 purging	closed	open	~2.2	3	400
IR measurement	open	open	< 0.05	~10[a]	-

[a]These values are the measurement times required to acquire background and difference IR spectra.

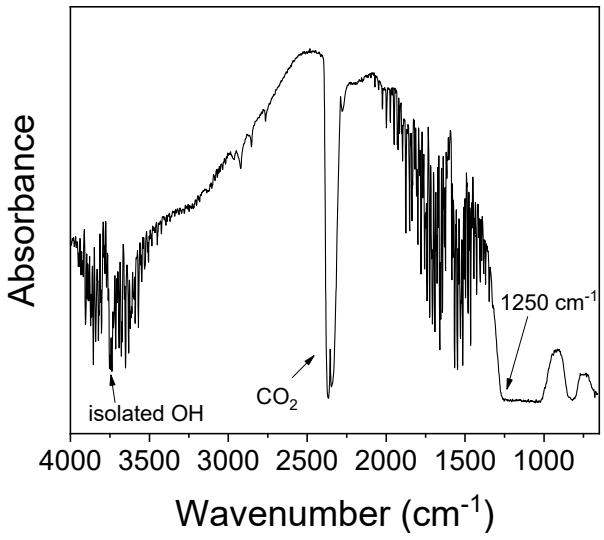

Figure S2. FTIR spectrum of a bare silica pellet which was used as a substrate in this work.

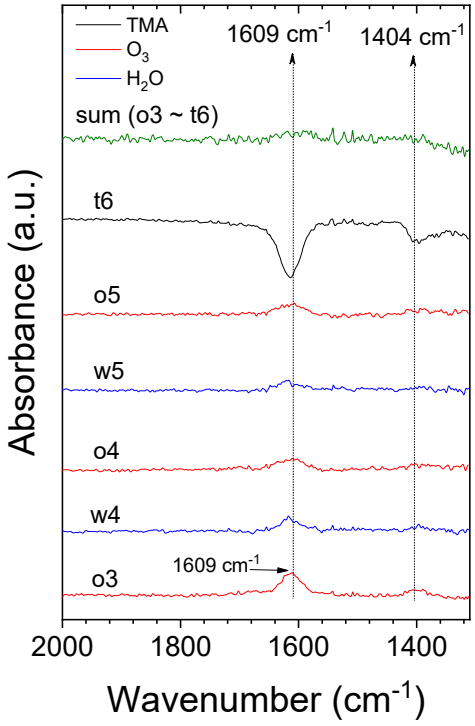

Figure S3. Magnified difference FTIR spectra selected from Fig. 3 (o3 to t6). The sum spectrum (green) was obtained by taking the sum of the other six difference spectra.

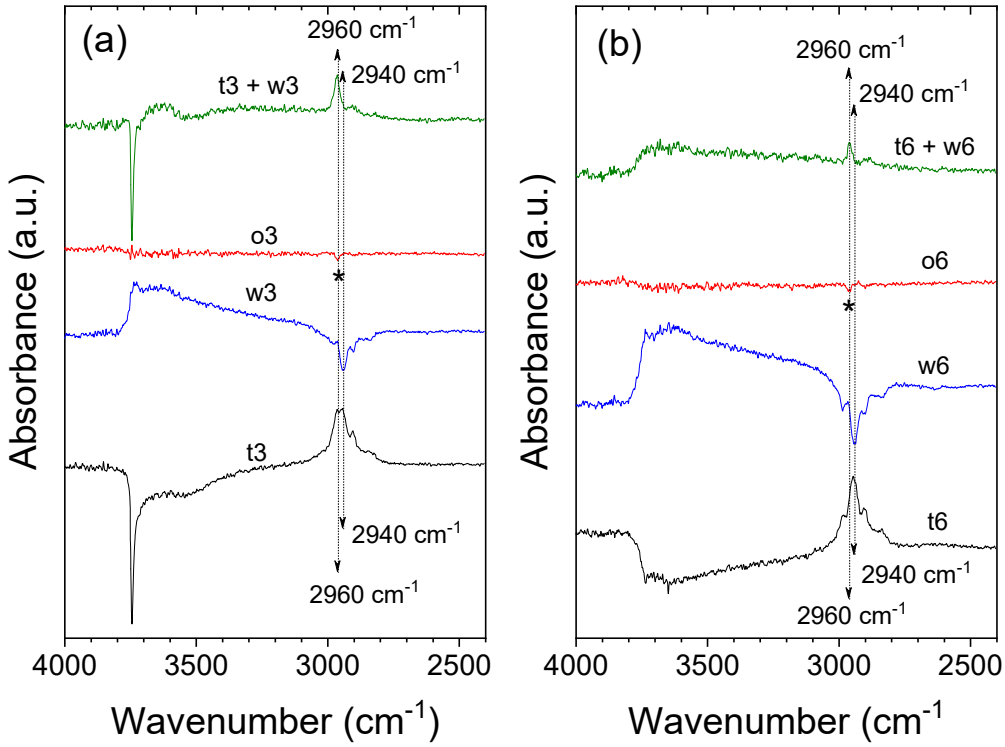

Figure S4. Extended difference (black, blue, and red) and sum (green) spectra of Fig. 4 including the OH stretching regions. The sum spectra (green) were obtained by taking the sum of the other two difference spectra (t3 + w3 (a); t6 + w6 (b)). The positive features in the methyl stretching regions of the sum spectra indicate the presence of the persistent methyl groups. The sharp negative feature in the OH stretching region of the sum spectrum (Fig. S4a) reveals that the isolated OH groups consumed by TMA exposure (t3) were not fully recovered by water exposure (w3).

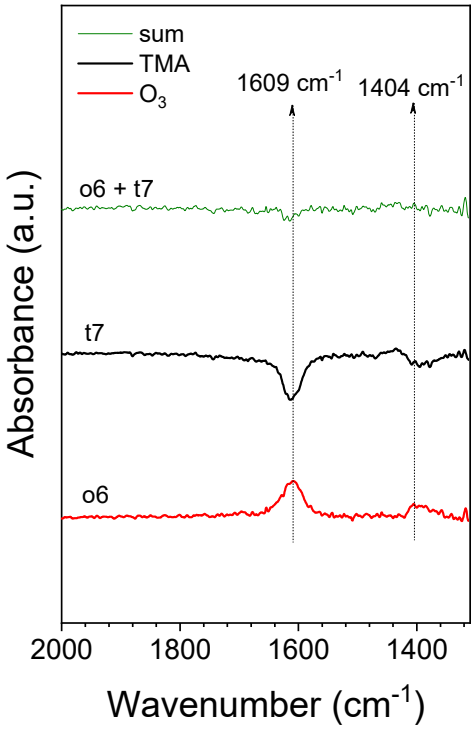

Figure S5. Magnified difference FTIR spectra selected from Fig. 3 (o6 to t7). The sum spectrum (green) was obtained by taking the sum of the difference spectra (o6 and t7).

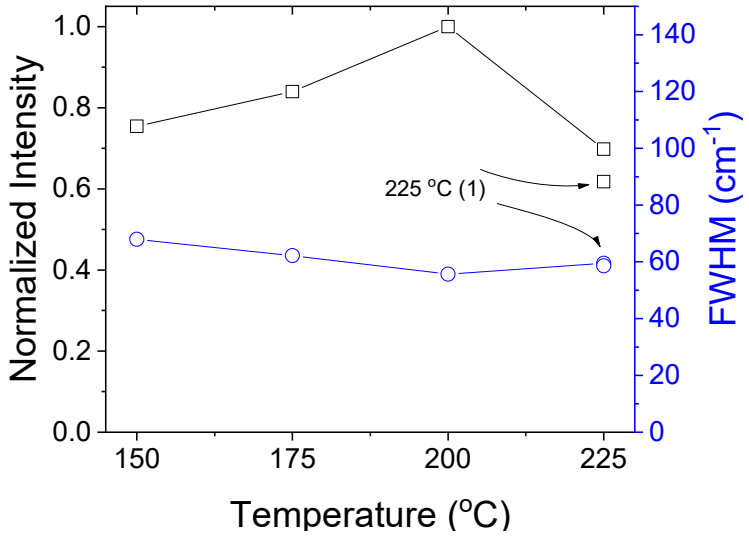

Figure S6. The normalized intensity and full width at half-maximum (FWHM) of the asymmetric stretching mode (~1609 cm^{-1}) of formate species formed by ozone exposures at various temperatures. These data were obtained from Fig. 6b.

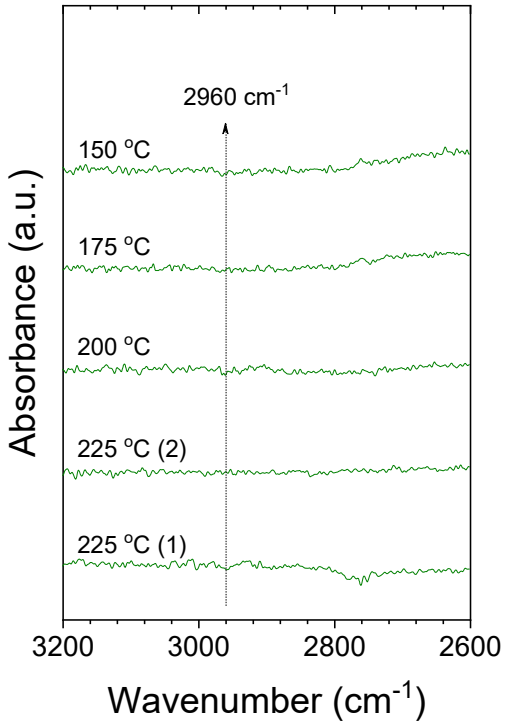

Figure S7. Sum FTIR spectra at each temperature obtained from Fig. 5a. Each sum spectrum was obtained by taking the sum of difference spectra of TMA, D_2O, and O_3 exposures at each temperature.

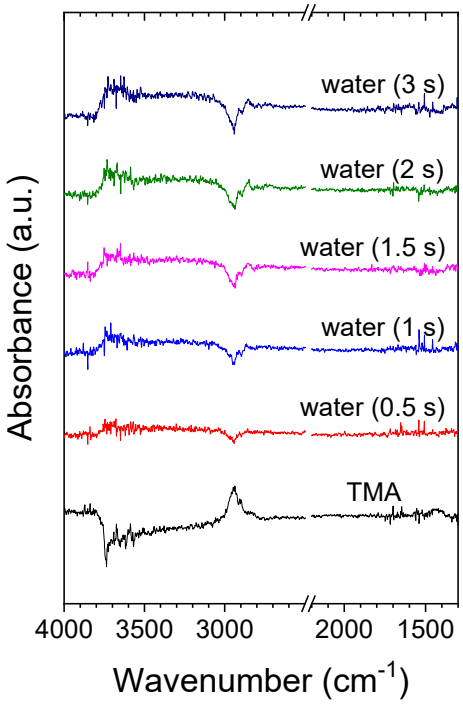

Figure S8. Difference FTIR spectra after exposures to TMA and water performed at 150 °C with various water exposure times. The difference spectra after exposure to water were referenced to the spectrum after exposure to TMA (10 torr and 10 min as list in Table S1). The difference spectrum after exposure to TMA was referenced to the spectrum of 20-cycled Al_2O_3.